Available online at www.sciencedirect.com
ScienceDirect
Journal of Molecular Catalysis A: Chemical 259 (2006) 84–90
JOURNAL OF MOLECULAR CATALYSIS A: CHEMICAL
www.elsevier.com/locate/molcata

Tertiary butylation of phenol over hexagonal *p6mm* mesoporous aluminosilicates with enhanced acidity

Jiahui Huang [a], Lihong Xing [a], Hongsu Wang [a], Gong Li [b], Shujie Wu [a], Tonghao Wu [a], Qiubin Kan [a,*]

[a] *Department of Chemistry, Jilin University, Changchun 130023, China*
[b] *Department of Chemical Engineering, Jiangsu Polytechnic University, Changzhou, Jiangsu 213016, China*

Received 18 October 2005; received in revised form 9 March 2006; accepted 7 June 2006
Available online 18 July 2006

Abstract

Through a two-step crystallization procedure and using cetyltrimethylammonium bromide (CTAB) as template, hexagonal *p6mm* mesoporous aluminosilicates (denoted as MB41) with n_{Si}/n_{Al} ratios from 15 to 50 have been assembled from the preformed zeolite Beta precursors under alkaline conditions. MB41 materials were characterized by powder XRD, N_2 adsorption–desorption, ^{27}Al-MAS NMR and pyridine adsorbed FT-IR spectroscopy techniques. Results obtained show that they are highly ordered hexagonal symmetry, and Al atoms are in tetrahedral coordination. Compared with classic Al-MCM-41, MB41 materials have stronger acidity, and also show significantly higher activities in the alkylation reaction of phenol with *tert*-butanol. At the reaction temperature of 145 °C, phenol conversion of 85.7% and 2,4-DTBP selectivity of 43.1% over MB41(25) are observed, but these over Al-MCM-41(25) are only 61.3% and 13.2%, respectively.

Keywords: MB41; Enhanced acidity; *tert*-Butylation of phenol; 4-TBP; 2,4-DTBP

1. Introduction

tert-Butylation of phenol is an industrially important reaction, and its products like 4-*tert*-butyl phenol (4-TBP) and 2,4-di-*tert*-butyl phenol (2,4-DTBP) are widely used as intermediates. Customarily 4-TBP is used to manufacture various antioxidants, varnish and lacquer resins, fragrances and protecting agents for plastics. 2,4-DTBP is mainly used to produce substituted triaryl phosphates [1,2]. This reaction is a typical Friedel–Crafts alkylation reaction, and can be catalyzed by a variety of acid catalysts like homogeneous Lewis acids [3] and Brönsted acids [4], and heterogeneous ion-exchange resins [5], zeolites [6] and mesoporous materials [7]. Use of homogeneous acid catalysts is generally avoided due to their unrecycled and corrosive nature, and ion-exchange resin cannot be used at high reaction temperature. Therefore, much attention of many research groups has been paid to the potential applications of microporous zeolites and mesoporous materials for their uniform pore sizes, high thermal stability and ability to be recycled. The catalytic activities of zeolites like H-Beta and HY in the alkylation reaction of phenol with *tert*-butanol have been investigated [6,8,9], and high conversion of phenol and selectivity to 4-TBP were observed. However, their small pore diameters in microporous region (<2 nm) severely limited the formation of bulky products like 2,4-DTBP. Since the discovery of mesoporous MCM-41S family [10,11], B, Al, Ga and Fe atoms have been successfully incorporated into the frameworks of mesoporous silicas by direct one-step synthesis or via postsynthesis modification for obtaining mesoporous solid acid catalysts. Their catalytic tests in the *tert*-butylation of phenol have also been extensively investigated [7,12–19]. Selvam and co-workers have reported that Al-MCM-41 and Fe-MCM-41 catalysts possessed moderate acidity and were appropriate for the selective synthesis of 4-TBP [7,16,19]. Later Hartmann and co-workers observed that FeAl-MCM-41 catalysts displayed higher conversion of phenol and selectivity to 4-TBP than Al-MCM-41 and Fe-MCM-41 catalysts [13]. However, due to the amorphous pore wall, the acidity of these mesoporous solid acid catalysts is much weaker than that of zeolites, and thus phenol conversion and 2,4-DTBP selectivity are very low. Therefore, attempts have been

* Corresponding author. Tel.: +86 431 8499140; fax: +86 431 8949334.
E-mail address: qkan@mail.jlu.edu.cn (Q. Kan).

1381-1169/$ – see front matter © 2006 Elsevier B.V. All rights reserved.
doi:10.1016/j.molcata.2006.06.001

made to synthesize new mesoporous materials with improved acidity.

By far improvedly acidic mesoporous materials like microporous–mesoporous composites [20–25], zeolite-coated mesostructures [26,27] and mesoporous materials assembled from preformed zeolite seeds [28–37] have been obtained. Due to the presence of microporous components, the acidity of microporous–mesoporous composites is improved. By recrystallization the pore walls of MCM-41 and HMS aluminosilicates in the presence of tetrapropylammonium cations, Kloetstra et al. [20] succeeded to improve their acidity and catalytic activities. Trong On et al. prepared zeolite-coated SBA-15 [26] and MCF (mesostructured cellular silica foams) [27] by impregnating them with a diluted clear solution containing primary zeolite units. These materials also present high acidity due to the presence of nanocrystalline zeolitic coating. Acidity improvement of mesoporous materials assembled from preformed zeolite seeds should be attributed to the presence of zeolite subunits. Liu and co-workers [28–30] utilized seeds of zeolite Y, ZSM-5 and Beta as precursors to synthesize steam-stable hexagonal mesoporous aluminosilicates. We have prepared enhancedly acidic cubic and hexagonal mesoporous aluminosilicates constructed of zeolite Beta precursors [36,37].

Alkylation reaction of phenol with *tert*-butanol has been performed by us to characterize the acidity of MB41 materials [36]. Herein the detailed studies of catalytic activities of MB41 materials under different reaction conditions have been carried out. In order to investigate the effect of both acidity and pore dimensions on the catalytic activities, amorphous mesoporous Al-MCM-41 and microporous zeolites like H-ZSM-5 and H-Beta have also been chosen as catalysts in this reaction. Due to the presence of the mesopore (>2 nm), MB41 catalysts display higher selectivity towards bulky 2,4-DTBP than microporous zeolites. Furthermore, MB41 catalysts have stronger acidity than classic Al-MCM-41, and hence show higher conversion of phenol and selectivity to 2,4-DTBP than amorphous Al-MCM-41 catalyst.

2. Experimental

2.1. Synthesis of MB41

A typical synthesis procedure of MB41 materials was as follows: 14.7 ml tetraethylammonium hydroxide aqueous solution (25.0 wt.%) and 2.25 ml 3.70 M HCl were mixed in a glass vessel, and then 2.5 g fumed silica was added under vigorous stirring. After vigorous stirring for 30 min, $NaAlO_2$ solution (required amount of sodium aluminate dissolved in 2.9 ml water) was added, and the reaction mixture was stirred until a homogeneous gel was obtained. The initial gel composition with molar ratio was: SiO_2:xAl_2O_3:0.028Na_2O:0.6TEAOH:0.2HCl:20H_2O (x = 0.01, 0.02 and 0.033). The gel was aged at 140 °C for 20 h under static condition, yielding zeolite Beta precursors. Then 9 ml aqueous solution of cetyltrimethylammonium bromide (19.3 wt.%) and 1.34 ml 3.70 M HCl were added to zeolite Beta precursors, and the final gel composition with molar ratio was SiO_2:xAl_2O_3:0.028Na_2O:0.6TEAOH:0.14CTMAB:0.36HCl:33H_2O (x = 0.01, 0.02 and 0.033). After stirring for 1 h, the mixture was transferred into a Teflon-lined stainless steel autoclave and aged at 140 °C for 24 h under static condition. After cooling down to room temperature, products were filtrated, washed with distilled water repeatedly and dried in air at ambient temperature. The template of as-synthesized MB41 samples was eliminated by calcination at 540 °C in flowing nitrogen for 2 h and then in flowing air for 8 h. Proton forms of MB41 materials were obtained from ion-exchange of NH_4NO_3, followed by calcination at 540 °C in flowing air for 4 h. In order to compare catalytic properties, Al-MCM-41, H-Beta and H-ZSM-5 with similar n_{Si}/n_{Al} ratio were also prepared according to the method described in Refs. [38–40].

2.2. Characterization

Powder X-ray diffraction (XRD) patterns were recorded on a Shimadzu XRD-6000 diffractometer system equipped with Ni-filtered Cu target Kα-ray (operation at 40 kV, 30 mA, wavelength λ = 0.15418 nm). Diffractions were carried out in the ranges (2θ): 1.5–10° and 10–50°, at the scanning speed of 1°/min and 2°/min, respectively. The n_{Si}/n_{Al} ratios of samples were measured by Perkin-Elmer 3300DV ICP. N_2 adsorption–desorption isotherms at 77 K were recorded with a Micromeritics ASAP 2020 system. Before measurements, samples were outgassed at 300 °C for 3 h. BET surface areas (S_{BET}) were calculated from adsorption branches in the relative pressure range of 0.05–0.20. Pore size distributions were calculated from adsorption branches by the Barret–Joyner–Halenda (BJH) method. The pore volume (V_p) was taken at the relative pressure of 0.989. ^{27}Al-MAS NMR spectra were measured on a Varian Unity-400 spectrometer, and chemical shifts were referenced to $Al(H_2O)_6^{3+}$. The measurements of mid-infrared spectra and IR spectra of pyridine adsorption were carried out on a Nicolet Avatar 370Dtgs spectrometer using KBr pellets and self-supporting pellets, respectively. Before the measurement of pyridine adsorption, the samples were pressed to thin wafers (10 mg/cm^2) and then placed into a quartz cell equipped with CaF_2 windows. Sample disks were evacuated at 400 °C for 2 h (10^{-5} Torr), and then cooled down to room temperature. After pyridine was adsorbed the infrared spectra were recorded at 150, 200 and 300 °C, respectively. Before NH_3-TPD measurements, samples were activated at 500 °C in pure nitrogen flow for 1 h, and then cooled down to 100 °C and began to adsorb ammonia. Physically adsorbed ammonia was removed by pure nitrogen flow at 100 °C. NH_3-TPD measurements were performed in the temperature range of 100–600 °C at an increasing temperature rate of 10 °C/min. Desorbed NH_3 was recorded continuously using a thermal conductivity cell, collected by a sulfuric acid (0.05 M) and quantitatively determined by titration using 0.1 M NaOH solution.

2.3. tert-Butylation of phenol

tert-Butylation of phenol was carried out in a continuous flow fixed quartz bed reactor (i.d. 6 mm) with N_2 as carrier gas. Prior to catalytic reaction, 0.5 g of catalyst was activated at 500 °C in N_2 for 1 h, and then the reactor was cooled to the required reaction temperature. The reaction mixture was injected from

Table 1
Textural properties of MB41 materials with different n_{Si}/n_{Al} ratios

Sample	MB41(50)	MB41(25)	MB41(15)	Al-MCM-41(25)
n_{Si}/n_{Al} (products)	49	24	16	25
a_0 (nm)[a] (as-synthesized)	5.00	5.22	5.24	5.10
a_0 (nm)[a] (calcined)	4.67	4.90	4.92	4.95
S_{BET} ($m^2\ g^{-1}$)	987	855	798	1206
V_p ($cm^3\ g^{-1}$)	0.89	0.74	0.62	1.04
D[b] (nm)	2.74	2.78	2.69	2.87
T[c] (nm)	1.93	2.12	2.23	2.08
Acid amount (mmol g^{-1})[d]	0.59	0.78	0.79	0.70

[a] Unit cell size, $a_0 = 2d_{100}/3^{1/2}$.
[b] Pore diameter (D).
[c] Pore wall thickness (T), $T = a_0$ (calcined) $- D$.
[d] Calculated from NH_3-TPD.

the top using a syringe pump. Alkylation reaction was investigated under different reaction temperature, $n_{tert\text{-butanol}}/n_{phenol}$ ratios and WHSV, etc. After the reaction was on for 2 h, products were collected and analyzed. Products were quantified by gas chromatography (GC-8A, Shimadzu) equipped with a XE60 capillary column, and confirmed by standard compounds.

3. Results and discussion

3.1. Synthesis and characterization of MB41

Through a two-step crystallization procedure, MB41 materials with different n_{Si}/n_{Al} ratios were hydrothermally synthesized. As shown in Table 1, the n_{Si}/n_{Al} ratios in gel are in close agreement with those in products. Powder XRD patterns of as-synthesized MB41 materials (Fig. 1A) display an intense (1 0 0) peak and two additional (1 1 0) and (2 0 0) peaks in the range of 1.5–10° (2θ), which are the characteristic peaks of hexagonal *p6mm* symmetry. In the range of 10–50° (2θ) only amorphous X-ray patterns are observed, indicating that MB41 samples are pure mesoporous phase without zeolite crystals. However, a vibrational band between 550 and 600 cm^{-1} can be observed in the IR spectrum of MB41(25), similar to that of zeolite Beta precursors with similar n_{Si}/n_{Al} ratio (Fig. 2). In contrast, this band is not obvious in the IR spectra of classic Al-MCM-41(25). A band

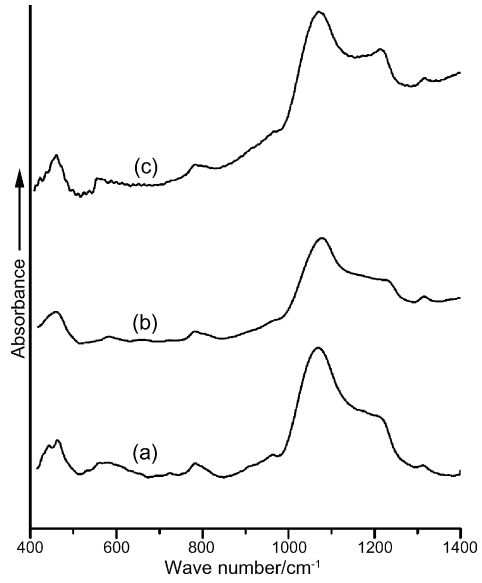

Fig. 2. IR spectra of MB41(25) (a), Al-MCM-41(25) (b) and zeolite Beta precursors with the n_{Si}/n_{Al} ratio of 25 (c).

near 550 cm^{-1} is actually characteristic of the five-membered rings of T–O–T (T = Si or Al) in zeolite crystals [29,41–44]. Thus, amorphous X-ray diffractions from 10° to 50° (2θ) and the presence of the band between 550 and 600 cm^{-1} prove that

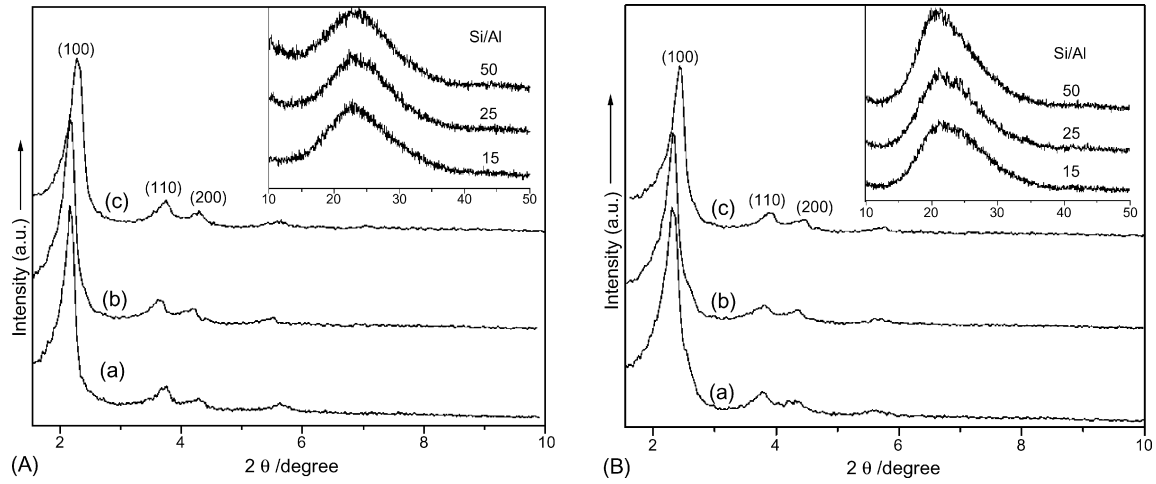

Fig. 1. Powder XRD patterns of as-synthesized MB41 (A) and calcined MB41 (B) with different n_{Si}/n_{Al} ratios: (a) 15, (b) 25 and (c) 50.

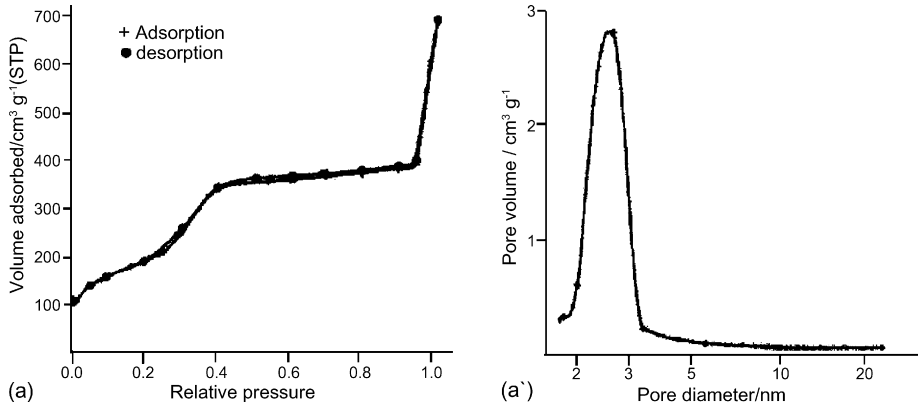

Fig. 3. N_2 adsorption–desorption isotherm (a) and pore size distribution (a′) of MB41(25).

the pore walls of MB41 contains zeolite Beta subunits. With the decreases of n_{Si}/n_{Al} ratios from 50 to 10, the shifts of the (1 0 0) peak to smaller angles are observed, suggesting the introduction of more aluminium atoms into the frameworks [45,46], and the cell parameters correspondingly increase (Table 1). After calcinations ordered hexagonal mesostructures are kept very well (Fig. 1B), but the cell parameters are reduced slightly (Table 1).

Nitrogen adsorption–desorption isotherm and the pore size distribution of the calcined MB41(25) are illustrated in Fig. 3. Typical IV isotherm with H1 type hysteresis loops is observed (Fig. 3a). The capillary condensation in the relative pressure range of 0.3–0.4 corresponds to framework mesopores, which are obtained after the elimination of template cetyltrimethylammonium bromide (CTAB). The sharp inflection in the relative pressure of 0.9–1.0 is attributed to the capillary condensation in the interparticle spaces. The pore size distribution (Fig. 3a′) suggests that MB41(25) has uniform mesoporous channels. Pore parameters of MB41 materials with different n_{Si}/n_{Al} ratios are shown in Table 1. With the increase of aluminium content in products, the pore volume and BET surface areas are correspondingly reduced, and pore walls are gradually thickened.

^{27}Al-MAS NMR spectra of the calcined MB41 samples and Al-MCM-41(25) are shown in Fig. 4. These spectra display a single resonance at ca. 54 ppm, indicating Al atoms in tetrahedral environment [45]. However, with the increase of aluminium content in MB41 materials, the signals are broaden and chemical shifts are slightly lowered, suggesting a possible distortion of aluminium in the framework. To estimate the type and strength of acid sites of MB41(25) and Al-MCM-41(25), infrared spectra of pyridine adsorption were used. In the IR spectra measured at 150 °C (Fig. 5a and d), the bands attributed to pyridine adsorbed on both Lewis acid sites (1455 and 1623 cm^{-1}) and Brönsted acid sites (1546 and 1638 cm^{-1}) and hydrogen-bonded pyridine (1447 and 1597 cm^{-1}) were observed, in addition, a band at 1491 cm^{-1} ascribed to pyridine associated with both Lewis and Brönsted acid sites was also observed [47]. The results indicate that MB41(25) and Al-MCM-41(25) have both Lewis and Brönsted acid sites. To evaluate to the strength of acidity, IR spectra of pyridine adsorption were measured at higher temperature. For both samples, with increasing the temperature from 150 to 300 °C all the bands become weaker, and even the bands due to hydrogen-bonded pyridine disappear (Fig. 5c and f). Furthermore, it is can also be observed that the bands attributed to both

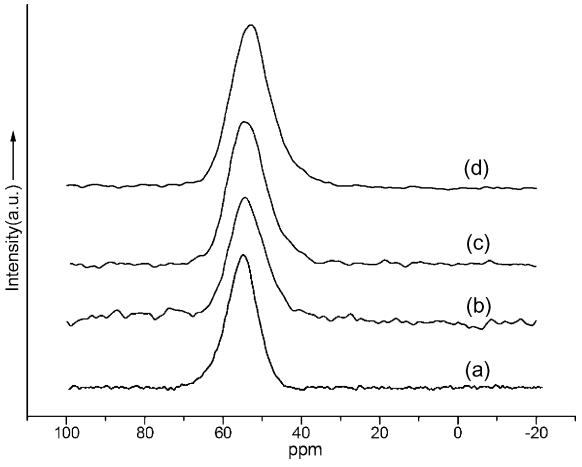

Fig. 4. ^{27}Al-MAS NMR patterns of the calcined samples: (a) Al-MCM-41(25), (b) MB41(50), (c) MB41(25) and (d) MB41(15).

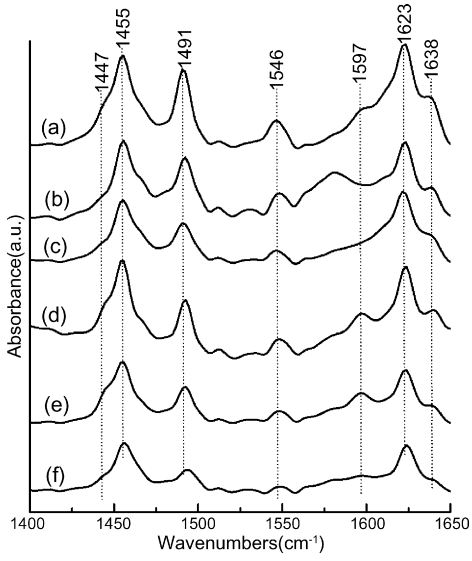

Fig. 5. IR spectra of pyridine adsorbed on MB41(25) at (a) 150 °C, (b) 200 °C, (c) 300 °C and on Al-MCM-41(25) at (d) 150 °C, (e) 200 °C and (f) 300 °C.

Lewis and Brönsted acid sites of MB41(25) are more intense than those of Al-MCM-41(25), which indicates that MB41(25) possesses larger amount of strong Lewis and Brönsted acid sites than classic Al-MCM-41(25).

3.2. Catalytic activity

Catalytic activities of MB41(25) and Al-MCM-41(25) catalysts at different reaction temperature are shown in Fig. 6 and Table 2. Products over both catalysts are 2-*tert*-butyl phenol (2-TBP), 4-*tert*-butyl phenol (4-TBP) and 2,4-di-*tert*-butyl phenol (2,4-DTBP), and a small amount of 2,4,6-tri-*tert*-butyl phenol (2,4,6-TTBP) is also observed over MB41(25). The highest conversions of phenol over both MB41(25) and Al-MCM-41(25) catalysts (85.7% and 61.3%, respectively) are observed at 145 °C (Fig. 6A and B), and above or below 145 °C phenol conversions decrease. This phenomenon has also been observed in the *tert*-butylation of phenol catalyzed by large pore zeolites [48]. In the temperature range of 105–185 °C, the main product over Al-MCM-41(25) is 4-TBP. With the increase of reaction temperature, the selectivity to 4-TBP correspondingly increases, and the highest selectivity to 4-TBP (91.5%) is obtained at 185 °C (Fig. 6B). The product distributions over MB41(25) vary with the changing of reaction temperature. Over 145 °C 4-TBP is the main product, but below 145 °C 2,4-DTBP, whose formation requires strong acidity [7], is the main product, and the highest selectivity to 2,4-DTBP (52.8%) is obtained at 125 °C. The difference of main products at the low temperature (<145 °C) over both catalysts should be attributed to that the acidity of MB41(25) is stronger than that of classic Al-MCM-41(25). The formation of small amount of more bulky 2,4,6-TTBP over MB41(25) catalyst also favors this viewpoint (Fig. 6A).

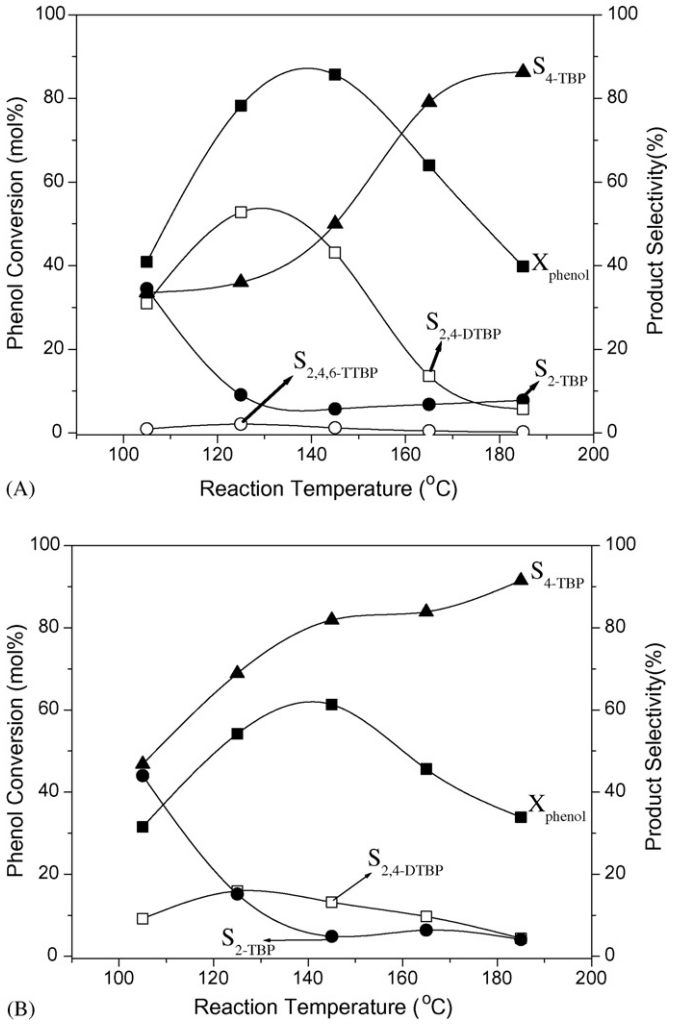

Fig. 6. Phenol conversion and products selectivities over (A) MB41(25) and (B) Al-MCM-41(25) (WHSV = 2.2 h^{-1}, $n_{tert\text{-butanol}}/n_{phenol}$ = 2.5, N_2 flow velocity = 20 ml/min, time-on-stream = 2 h).

MB41(15) and MB41(50) catalysts have also been tested in the *tert*-butylation reaction of phenol (Table 2), and display similar catalytic activities in comparison to MB41(25). With the decrease of n_{Si}/n_{Al} ratios, phenol conversion and 2,4-DTBP and 2,4,6-TTBP selectivities slightly increase, consistent with the increase of their acid amount (Table 1). In order to investigate the effect of pore dimensions on the conversion of phenol and products selectivities, microporous zeolites H-Beta(25) and H-ZSM-5(25) are also chosen as catalysts, and their catalytic activities are shown in Table 2. The pore size of H-ZSM-5(25) is about 0.55 nm, nearly equivalent to the molecule size of phenol, and hence it is very difficult for phenol molecules to enter microporous channels, and only the acidic sites on the external area can be easily reached. However, the external area of H-ZSM-5(25) is very small, therefore, low phenol conversion (16.2%) is obtained. The pore size of H-Beta(25) is about 0.75 nm, and large enough for phenol molecules to enter the channels and react with *tert*-butanol over the acidic sites. High phenol conversion of 92.1% and 4-TBP selectivity of 76.6% are obtained. But the selectivity to bulky 2,4-DTBP is still low (20.3%), and more bulky 2,4,6-TTBP is not observed, indicating that the pore dimension of H-Beta(25) is still not large enough. Therefore, larger pore size is required for the formation of bulky 2,4-DTBP and 2,4,6-TTBP. Classic Al-MCM-41(25) has the pore channels in the mesoporous range (>2 nm), but its catalytic activity is still very low (Table 2), which should be attributed to its weak acidity. Therefore, it is believed that in this reaction the conversion of phenol and product distribution mainly rely on the acidity and pore structure of solid catalyst, and stronger acidity and larger pore size favor higher phenol conversion and 2,4-DTBP selectivity. MB41(25) catalyst possesses both mesopore channels and enhanced acidity, and hence displays high phenol conversion and 2,4-DTBP selectivity (Table 2). Further detailed catalytic tests of MB41(25) under different WHSV, $n_{tert\text{-butanol}}/n_{phenol}$ ratios and reaction time have also been carried out.

Effect of WHSV on phenol conversion and products selectivities is shown in Fig. 7. With the decrease of WHSV from 11.0 to 1.37 h^{-1} phenol conversion increases from 42.9% to 95.3%, implying that longer contact time (i.e. more adsorption of *tert*-butanol molecules on the Brönsted acid sites) favors the alkylation reaction. At the same time, the selectivity to 2-TBP decreases, and that to 2,4-DTBP increases, and high 2,4-DTBP selectivity of 58.7% can be obtained at WHSV of 1.37 h^{-1}. Therefore, by reducing the WHSV, high conversion of phenol and selectivity to 2,4-DTBP can be obtained.

Table 2
Catalytic activity and product distribution[a]

	Catalysts					
	Al-MCM-41(25)	MB41(50)	MB41(25)	MB41(15)	H-Beta(25)	H-ZSM-5(25)
Phenol conversion (mol%)	61.3	72.5	85.7	87.3	92.1	16.2
Product selectivity in alkyl phenol (mol%)						
2-TBP	4.9	7.7	5.7	4.6	3.1	34.1
4-TBP	81.9	52.3	50.0	49.2	76.6	43.6
2,4-DTBP	13.2	39.1	43.1	44.3	20.3	22.3
2,4,6-TTBP	–	0.9	1.2	1.9	–	–

[a] Reaction temperature = 145 °C; $n_{tert\text{-butanol}}/n_{phenol}$ = 2.5; WHSV = 2.2 h^{-1}; time-on-stream = 2 h; N_2 flow velocity = 20 ml/min.

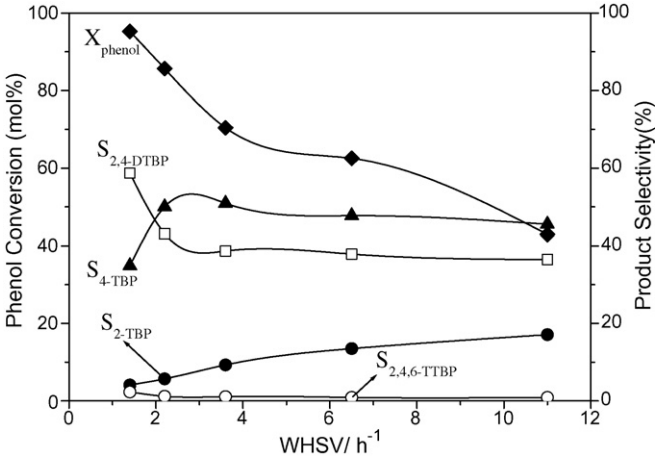

Fig. 7. Effect of WHSV on phenol conversion and products selectivities over MB41(25) ($n_{tert\text{-butanol}}/n_{phenol}$ = 2.5; reaction temperature = 145 °C; N_2 flow velocity = 20 ml/min; time-on-stream = 2 h).

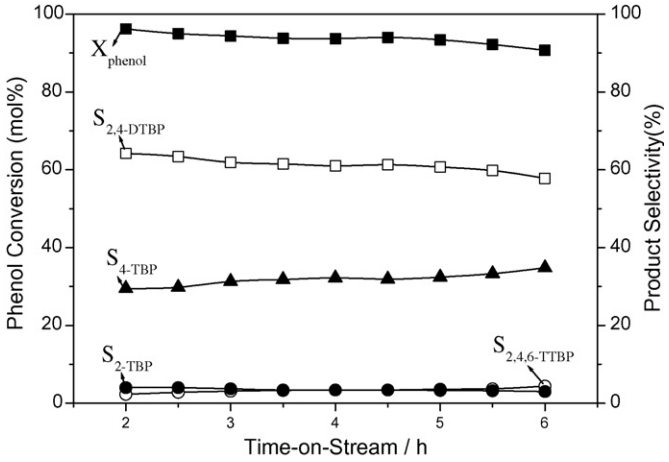

Fig. 9. Effect of time-on-stream on phenol conversion and products selectivities over MB41(25) (WHSV = 2.2 h^{-1}; reaction temperature = 145 °C; N_2 flow velocity = 10 ml/min; $n_{tert\text{-butanol}}/n_{phenol}$ = 4).

Phenol conversion and products selectivities over MB41(25) are also affected by the molar feed ratios (Fig. 8). It is observed that phenol conversion increases from 69.9% to 96.2% with increasing the $n_{tert\text{-butanol}}/n_{phenol}$ ratio from 1.0 to 4.0, and abrupt increase is present when *tert*-butanol to phenol ratio increases from 1.0 to 1.75. Due to the competition of polar molecules *tert*-butanol with phenol for adsorption sites, higher content of *tert*-butanol leads to the formation of more olefins by the dehydration, and then higher phenol conversion is obtained. Similar results have been reported before [12,49,50]. Likewise, the selectivity to 2,4-DTBP increases, indicating that the increase of the content of *tert*-butanol promotes further alkylation of monoalkylated products (2-TBP and 4-TBP) to 2,4-DTBP (Fig. 8).

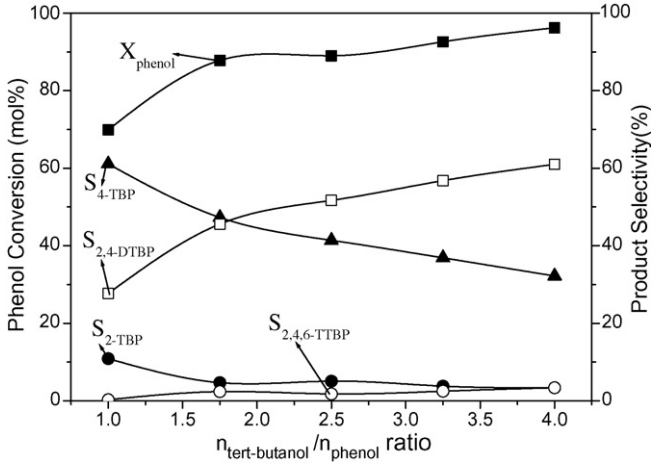

Fig. 8. Effect of $n_{tert\text{-butanol}}/n_{phenol}$ ratio on phenol conversion and products selectivities over MB41(25) (WHSV = 2.2 h^{-1}, reaction temperature = 145 °C, N_2 flow velocity = 10 ml/min, time-on-stream = 2 h).

From the discussion above, the relative optimal reaction condition is temperature of 145 °C, WHSV of 2.2 h^{-1} and $n_{tert\text{-butanol}}/n_{phenol}$ ratio of 4. Effect of time-on-stream on phenol conversion and product selectivities is investigated under this condition (Fig. 9). Excellent catalytic activity of MB41(25) with exceptionally high phenol conversion of 96.2% and 2,4-DTBP selectivity of 64.2% is observed when the reaction is on for 2 h. After further reaction for another 4 h, a slight deactivation of MB41(25) is observed, and phenol conversion and 2,4-DTBP selectivity decrease to 90.7% and 57.8%, respectively. The results might be attributed to the decrease of the amount of strong acid sites. After longer time of reaction, some strong acid sites are blocked by coke, and thus the formation of bulky 2,4-DTBP is suppressed because its formation requires strong acid sites. At the same time, the decrease of total acid amount of MB41(25) leads to the decrease of phenol conversion. It has been reported that at high reaction temperature (higher than 250 °C), phenol conversion over ZnAl-MCM-41

and FeAl-MCM-41 catalysts drastically decreased with reaction time [12,13]. Slight deactivation of MB41(25) should be attributed to the relative low reaction temperature (145 °C).

4. Conclusions

Templated by cetyltrimethylammonium bromide (CTAB), MB41 materials with different n_{Si}/n_{Al} ratios have been hydrothermally synthesized through the self-assembly of preformed zeolite Beta precursors. MB41 samples were characterized by powder XRD, N_2 adsorption–desorption, ^{27}Al-MAS NMR and pyridine adsorbed FT-IR spectroscopy techniques. Analytic results show that MB41 materials are ordered hexagonal *p*6*mm* mesostructures, and have stronger acidity than classic Al-MCM-41(25). In the *tert*-butylation of phenol, MB41(25) and MB41(15) display significantly higher catalytic activities than classic Al-MCM-41(25), and even MB41(50), whose acid amount is smaller than that of Al-MCM-41(25), shows higher phenol conversion and 2,4-DTBP selectivity. In the further catalytic tests under different conditions, MB41(25) catalyst displays excellent catalytic performances.

Acknowledgements

We thank the National Basic Research Program of China (2004CB217804) and Jilin province (20020806) for the financial support of this work.

References

[1] A. Knop, L.A. Pilato, Phenolic Resin Chemistry, Springer, Berlin, 1985.
[2] A.J. Kolka, J.P. Napolitano, G.G. Elike, J. Org. Chem. 21 (1956) 712.
[3] G. Sartori, F. Bigi, G. Casiraghi, G. Carnati, L. Chiesi, A. Arduini, Chem. Ind. 22 (1985) 762.
[4] A.A. Carlton, J. Org. Chem. 13 (1948) 120.
[5] K.G. Chandra, M.M. Sharma, Catal. Lett. 19 (1993) 309.
[6] A.V. Krishnan, K. Ojha, N.C. Pradhan, Org. Process Res. Dev. 6 (2002) 132.
[7] A. Sakthivek, S.K. Badamali, P. Selvam, Microporous Mesoporous Mater. 39 (2000) 457.
[8] K. Zhang, C. Huang, H. Zhang, S. Xiang, S. Liu, D. Xu, H. Li, Appl. Catal. A 166 (1998) 89.
[9] R. Anand, R. Maheswari, K.U. Gore, B.B. Tope, J. Mol. Catal. A 193 (2003) 251.
[10] C.T. Kresge, M.E. Leonowicz, W.J. Roth, J.C. Vartuli, J.S. Beck, Nature 359 (1992) 710.
[11] J.S. Beck, J.C. Vartuli, W.J. Roth, M.E. Leonowicz, C.T. Kresge, K.D. Schmitt, C.T.W. Chu, D.H. Olson, E.W. Sheppard, S.B. McCullen, J.B. Higgins, J.L. Schlenker, J. Am. Chem. Soc. 114 (1992) 10834.
[12] R. Savidha, A. Pandurangan, M. Palanihamy, V. Murugesan, J. Mol. Catal. A 211 (2004) 165.
[13] A. Vinu, K.U. Nandhini, V. Murugesan, W. Bohlmann, V. Umamaheswari, A. Poppl, M. Hartmann, Appl. Catal. A 265 (2004) 1.
[14] A. Sakthivel, S.E. Dapurkar, N.M. Gupta, S.K. Kulshreshtha, P. Selvam, Microporous Mesoporous Mater. 65 (2003) 177.
[15] P. Selvam, S.E. Dapurkar, Catal. Today 96 (2004) 135.
[16] S.K. Badamali, A. Sakthivel, P. Selvam, Catal. Lett. 65 (2000) 153.
[17] A. Sakthivel, P. Selvam, Catal. Lett. 84 (2002) 37.
[18] S.K. Badamali, A. Sakthivel, P. Selvam, Catal. Today 63 (2000) 291.
[19] A. Sakthivel, N. Saritha, P. Selvam, Catal. Lett. 72 (2001) 225.
[20] K.R. Kloetstra, H. van Bekkum, J.C. Jansen, Chem. Commun. (1997) 2281.
[21] A. Karlsson, M. Stocker, R. Schmidt, Microporous Mesoporous Mater. 27 (1999) 181.
[22] L. Huang, W. Guo, P. Deng, Z. Xue, Q. Li, J. Phys. Chem. B 104 (2000) 2817.
[23] Y. Xia, R. Mokaya, J. Mater. Chem. 14 (2004) 863.
[24] W. Guo, C. Xiong, L. Huang, Q. Li, J. Mater. Chem. 11 (2001) 1886.
[25] W. Guo, L. Huang, P. Deng, Z. Xue, Q. Li, Microporous Mesoporous Mater. 44/45 (2001) 427.
[26] D. Trong On, S. Kaliaguine, Angew. Chem. Int. Ed. 41 (2002) 1036.
[27] D. Trong On, S. Kaliaguine, J. Am. Chem. Soc. 125 (2003) 618.
[28] Y. Liu, W. Zhang, T.J. Pinnavaia, J. Am. Chem. Soc. 122 (2000) 8791.
[29] Y. Liu, W. Zhang, T.J. Pinnavaia, Angew. Chem. Int. Ed. 40 (2001) 1255.
[30] Y. Liu, J. Pinnavaia, Chem. Mater. 14 (2002) 3.
[31] Z.T. Zhang, Y. Han, L. Zhu, R. Wang, Y. Yu, S. Qiu, D. Zhao, F. Xiao, Angew. Chem. Int. Ed. 40 (2001) 1258.
[32] Z.T. Zhang, Y. Han, F. Xiao, S. Qiu, L. Zhu, R. Wang, Y. Yu, Z. Zhang, B. Zou, Y. Wang, H. Sun, D. Zhao, Y. Wei, J. Am. Chem. Soc. 123 (2001) 5014.
[33] Y. Han, S. Wu, Y. Sun, D. Li, F. Xiao, Chem. Mater. 14 (2002) 1144.
[34] Y. Han, F. Xiao, S. Wu, Y. Sun, X. Meng, D. Li, S. Lin, J. Phys. Chem. B 105 (2001) 7963.
[35] Y. Han, N. Li, L. Zhao, D. Li, X. Xu, S. Wu, Y. Di, C. Li, Y. Zou, Y. Yu, F. Xiao, J. Phys. Chem. B 107 (2003) 7551.
[36] J. Huang, G. Li, S. Wu, H. Wang, L. Xing, K. Song, T. Wu, Q. Kan, J. Mater. Chem. 15 (2005) 1055.
[37] G. Li, Q. Kan, T. Wu, C. Hou, F. Xiao, J. Huang, Stud. Surf. Sci. Catal. 146 (2003) 149.
[38] G. Li, Q. Kan, H. Zhang, T. Wu, Petrochem. Technol. 31 (2002) 104 (in Chinese).
[39] T. Song, L. Liu, R. Xu, Cuihua Xuebao 12 (1991) 283.
[40] Q. Zhou, W. Pang, S. Qiu, M. Jia, CN Pat. ZL 93117593.3, 1996; Q. Zhou, B. Li, S. Qiu, W. Pang, Chem. J. Chin. Univ. 20 (1999) 693.
[41] P.A. Jacobs, E.G. Derouane, J. Weitkamp, J. Chem. Soc. Chem. Commun. (1981) 591.
[42] J.C. Jansen, F.J.V. Gaag, H.V. Bekkum, Zeolites 4 (1984) 369.
[43] B.J. Schoeman, Stud. Surf. Sci. Catal. 105 (1997) 647.
[44] C.E.A. Kirschhock, R. Ravishankar, F. Verspeurt, P.J. Grobet, P.A. Jacobs, J.A. Martens, J. Phys. Chem. B 103 (1999) 4965.
[45] K.M. Reddy, C. Song, Catal. Lett. 36 (1996) 103.
[46] R.B. Borade, A. Clearfield, Catal. Lett. 31 (1995) 267.
[47] E.P. Parry, J. Catal. 2 (1963) 371.
[48] K. Zhang, H. Zhang, G. Xu, S. Xiang, D. Xu, S. Liu, H. Li, Appl. Catal. A: Gen. 207 (2001) 183.
[49] R.F. Parton, J.M. Jacobs, H.V. Ootehem, P.A. Jacobs, Stud. Surf. Sci. Catal. 46 (1988) 211.
[50] S. Subramanian, A. Mitra, C.V.V. Satyanarayana, D.K. Chakrabarty, Appl. Catal. A 159 (1997) 229.